



**HAL**  
open science

## Optimization of thermopressing conditions for the production of binderless boards from a coriander twin-screw extrusion cake

Evelien Uitterhaegen, Laurent Labonne, Othmane Merah, Thierry Talou, Christine Ballas, Thierry Véronèse, Philippe Evon

► **To cite this version:**

Evelien Uitterhaegen, Laurent Labonne, Othmane Merah, Thierry Talou, Christine Ballas, et al.. Optimization of thermopressing conditions for the production of binderless boards from a coriander twin-screw extrusion cake. *Journal of Applied Polymer Science*, 2017, vol. 134 (n° 13), pp. 44650. 10.1002/app.44650 . hal-01416004

**HAL Id: hal-01416004**

**<https://hal.science/hal-01416004>**

Submitted on 6 Jan 2022

**HAL** is a multi-disciplinary open access archive for the deposit and dissemination of scientific research documents, whether they are published or not. The documents may come from teaching and research institutions in France or abroad, or from public or private research centers.

L'archive ouverte pluridisciplinaire **HAL**, est destinée au dépôt et à la diffusion de documents scientifiques de niveau recherche, publiés ou non, émanant des établissements d'enseignement et de recherche français ou étrangers, des laboratoires publics ou privés.



## Open Archive TOULOUSE Archive Ouverte (OATAO)

OATAO is an open access repository that collects the work of Toulouse researchers and makes it freely available over the web where possible.

This is an author-deposited version published in : <http://oatao.univ-toulouse.fr/>  
Eprints ID : 17380

**To link to this article** : DOI : 10.1016/app.44650  
URL : <http://dx.doi.org/10.1002/app.44650>

**To cite this version** : Uitterhaegen, Evelien and Labonne, Laurent and Merah, Othmane and Talou, Thierry and Ballas, Stéphane and Véronèse, Thierry and Evon, Philippe *Optimization of thermopressing conditions for the production of binderless boards from a coriander twin-screw extrusion cake*. (2017) Journal of Applied Polymer Science, vol. 134 (n° 13). pp. 44650. ISSN 0021-8995

Any correspondence concerning this service should be sent to the repository administrator: [staff-oatao@listes-diff.inp-toulouse.fr](mailto:staff-oatao@listes-diff.inp-toulouse.fr)

# Optimization of thermopressing conditions for the production of binderless boards from a coriander twin-screw extrusion cake

E. Uitterhaegen,<sup>1</sup> L. Labonne,<sup>1</sup> O. Merah,<sup>1</sup> T. Talou,<sup>1</sup> S. Ballas,<sup>2</sup> T. Véronèse,<sup>2</sup> Ph. Evon<sup>1</sup>

<sup>1</sup>Laboratoire de Chimie Agro-industrielle (LCA), Université de Toulouse, INRA, INPT, Toulouse, France

<sup>2</sup>Ovalie Innovation, Auch 32000, France

Correspondence to: Ph. Evon (E-mail: philippe.evon@ensiacet.fr)

**ABSTRACT:** A deoiled press cake resulting from twin-screw extrusion of coriander fruits was used as a raw material for the production of self-bonded boards. The operating parameters for thermopressing were varied and include the applied pressure (19.6–39.2 MPa), molding time (60–300 s), and molding temperature (155–205 °C). The optimized process conditions (21.6 MPa, 300 s, 205 °C) resulted in a board with a density of 1323 kg/m<sup>3</sup>, a flexural strength of 23 MPa, a modulus of elasticity of 4.4 GPa, and a thickness swelling of 31%. The thickness swelling was effectively reduced to 20% through the application of a heat treatment at 200 °C after thermopressing. A variation of the moisture content of the press cake between 3 and 8% showed that increased moisture contents do not lead to improved mechanical properties of the resulting board and further induce internal fracturing of the board during thermopressing. The manufactured binderless boards may act as environmentally friendly alternatives to commercial wood-based boards such as oriented strand board and particleboard. © 2016 Wiley Periodicals, Inc. *J. Appl. Polym. Sci.* **2016**, *133*, 44650.

**KEYWORDS:** mechanical properties; molding; proteins; swelling; thermal properties

**DOI:** 10.1002/app.44650

## INTRODUCTION

The steady depletion of petroleum and changes in the world forest resource, together with a continuously growing population and prominent environmental concerns and regulations, have driven the materials industry toward the implementation of more sustainable products and processes. In view of this, there is an ongoing search for alternative sources of lignocellulosic fibers. It is, however, of vital importance that the resulting products can be competitive with classic materials of a non-renewable nature in terms of mechanical properties, durability, and cost.

Here, an interesting approach could be to focus on lignocellulosic by-products from the processing of agricultural raw materials, which show both a low cost and high availability. Furthermore, it has been shown that thermopressing of lignocellulosic waste products such as wheat straw,<sup>1</sup> sugarcane bagasse,<sup>2</sup> and oil palm trunk<sup>3</sup> allow the production of binderless boards by the use of heat or steam treatments or compression. This eliminates the necessity of using synthetic adhesives such as formaldehyde resins that often make up for more than half of the board production costs, imply a significant environmental burden, and may even show adverse human health effects.<sup>4</sup> These materials could present competitive wood supplements in the wood-based industry, as they are economical and show

attractive mechanical properties, environmental friendliness, and a simple production process.<sup>5</sup>

Recently, researchers have focused on the use of oilseed press cakes for the production of biodegradable, renewable boards. Press cakes are abundantly available as by-products from the vegetable oil industry and are often used in the feed industry or as an energy source. The fabrication of materials may present an application with high added value. It has been shown that components such as proteins and lignins can act as natural binders, leading to the production of cohesive binderless boards, while at the same time, lignocellulosic fibers can act as reinforcing fillers, enhancing mechanical properties.<sup>6,7</sup> Effective production of self-bonded boards has been accomplished from sunflower cake,<sup>8</sup> jatropha cake,<sup>9,10</sup> coriander cake,<sup>11</sup> and castor cake.<sup>12</sup>

Coriander (*Coriandrum sativum* L.) is an annual herb from the Apiaceae family that is mainly produced in India with an annual production of around 500,000 tons.<sup>13</sup> The fruits contain a significant amount of vegetable oil between 20 and 28%, as well as an essential oil fraction of 0.3–0.9%.<sup>14</sup> Coriander vegetable oil has been shown to be particularly rich in phytosterols (about 670 mg/100 g) and petroselinic acid (around 73% of all fatty acids), an uncommon positional isomer of oleic acid with interesting anti-inflammatory and anti-aging properties.<sup>15–17</sup> The vegetable oil has recently been labeled as a Novel Food

Ingredient (NFI) and may be consumed as a food supplement.<sup>18</sup> Further, a recent study has shown that there is a co-extraction of vegetable and essential oil during continuous pressing of the coriander fruits in a twin-screw extruder, resulting in agreeably scented vegetable oil.<sup>19</sup> Therefore, coriander oil has recently gained considerable interest from the food, cosmetic, and chemical industry.

In the context of sustainability and the valorization of by-products, this study focuses on the use of a coriander press cake for the manufacture of self-bonded boards, further enhancing the concept of a coriander biorefinery. The cake used in this study resulted from an optimized twin-screw extrusion process of coriander fruits for vegetable oil extraction through mechanical pressing. The extrusion process resulted in an oil recovery of 52%, further rendering a press cake with a residual oil content of 13% of the dry matter. A previous study dealing with the production of binderless boards from a sunflower cake originating from the whole plant revealed that complete deoiling of the cake before thermopressing results in important improvements of the mechanical properties of the resulting boards.<sup>20</sup> This may be explained by the presence of defects in boards produced from a non-deoiled cake, which result from the expression of oil during thermopressing. Therefore, the obtained press cake was further deoiled through solvent extraction prior to thermopressing.

The only previous study dealing with the production of self-bonded boards from coriander material involves a press cake resulting from single-screw extrusion and containing about 17% of residual oil.<sup>11</sup> A significant expression of oil was observed during thermopressing, representing about 50% of the residual oil in the press cake. Thermopressing conditions that resulted in the board with the highest mechanical resistance (11.3 MPa flexural strength, 2.6 GPa modulus of elasticity, 70 Shore D surface hardness) included a mold temperature of 200 °C, an applied pressure of 36.8 MPa, and a molding time of 3 min. The board showed high water sensitivity with 33% water absorption and 51% thickness swelling and this is a well-known problem for boards produced from lignocellulosic material and may result in reduced mechanical properties and dimensional stability.<sup>21</sup>

This study aims to obtain novel self-bonded boards from a deoiled twin-screw extrusion coriander press cake with enhanced mechanical properties and water sensitivity. First, it comprises a complete characterization of the starting material, which is of key importance for further understanding of the material behavior under thermopressing conditions, especially the bonding mechanism. Second, an analysis of the influence of thermopressing conditions (temperature, pressure, and time) on the mechanical resistance (flexural properties, surface hardness, and impact strength), the water sensitivity, and color characteristics of the resulting boards was carried out. This will allow the establishment of a prediction model through regression analysis, which is very useful from an industrial point of view. Furthermore, from this, optimal conditions may be calculated which would lead to the production of a board with maximized mechanical properties. Finally, the influence of the moisture content of the starting material on the properties of the resulting boards and the effectiveness

**Table I.** Composition of the Deoiled Coriander Press Cake

Component	Content (% db)
Cellulose	34.7 ± 0.4
Hemicelluloses	36.9 ± 0.9
Lignins	1.0 ± 0.1
Proteins	26.7 ± 0.1
Lipids	0.9 ± 0.3
Minerals	6.7 ± 0.4

of surface treatments of the binderless boards to improve water sensitivity were evaluated.

## EXPERIMENTAL

### Material

Coriander fruits of French origin (GSN maintenaire variety) were supplied by GSN Semences (Le Houga, France) and subjected to twin-screw extrusion for vegetable oil extraction. Pressing was carried out with a Cleextral (Firminy, France) BC 21 twin-screw extruder of which the screw profile was the optimal one determined by Uitterhaegen *et al.* for coriander fruits.<sup>19</sup> The applied operating conditions consisted of a screw speed of 100 rpm, a seed inlet flow rate of 3.5 kg dry matter/h, and an extrusion temperature of 65 °C near the trituration zone and 74 °C near the pressing zone. The obtained press cake was further deoiled through a 5 h solvent extraction using a 1 L Soxhlet apparatus and cyclohexane as the extracting solvent. The deoiled press cake composition is presented in Table I.

### Analytical Methods

The moisture content, mineral content, and residual oil content were determined according to ISO 665:2000, 749:1977, and 659:2009, respectively.<sup>22–24</sup> The cellulose, hemicelluloses, and lignins content were determined by the use of the acid detergent fiber-neutral detergent fiber (ADF-NDF) method of Van Soest and Wine.<sup>25,26</sup> The protein content was determined according to ISO 5983-1:2005.<sup>27</sup>

### Optical Granulometry

The particle size distribution of the deoiled press cake was determined through optical microscopy. For this, a Nacet France Z 45 P (Dijon, France) ×15 binocular magnifier was used and five different photographs were taken by the use of the Archimed 4.0 (Lille, France) software. Next, the particle size distribution and mean particle diameter were determined through measurements of the particle diameters on the five photographs by the use of the ImageJ (National Institutes of Health, Bethesda, MD, USA) software.

### Thermogravimetric Analysis

A Thermogravimetric analysis (TGA) was carried out by the use of a Shimadzu TGA-50 (Kyoto, Japan) analyzer. Dynamic analysis was conducted under air from 20 to 750 °C, with a heating rate of 5 °C/min. Material was conditioned in a climatic chamber (25 °C, 60% RH) for 3 weeks prior to analysis. Test samples comprised about 5 mg of material. Sample weight was measured as a function of temperature and results are presented as the percentage of non-degraded sample ( $1 - D$ , %), where

$D = (W_0 - W)/W_0$  and  $W_0$  and  $W$  are the sample weight at start and during analysis. The analysis was carried out in duplicate.

### Differential Scanning Calorimetry

Differential scanning calorimetry (DSC) was conducted with a Mettler Toledo DSC 1 STARe system (Columbus, OH, USA) power compensation calorimeter, equipped with an IntraCooler cooling system. Nitrogen was used as the purge gas with a flow rate of 50 mL/min. Prior to analysis, calibration of temperature and energy was carried out using zinc, indium, and distilled water, which show transition temperatures of 419.5 °C, 156.6 °C, and 0 °C, respectively. Analyses were conducted with hermetic 120  $\mu$ L stainless steel capsules with O-rings resistant to internal pressures of 20 bar. A heating rate of 5 °C/min was applied, from 25 °C to 250 °C. Test samples consisted of about 10 mg of material. Data analysis was carried out by the use of the STARe software (Mettler Toledo, Columbus, OH, USA).

### Thermopressing

Molding of the material was carried out through thermopressing in a 150 mm  $\times$  150 mm aluminum mold. For this, a Pine-tte Emidecau Industries (Chalon-sur-Saône, France) heated hydraulic press with a capacity of 400 tons was used. For all optimization trials, the deoiled cake was dried for 12 h at 50 °C in a ventilated oven, resulting in a moisture content of  $3.1 \pm 0.1\%$ . As such, vapor generation during thermopressing is minimized, which might otherwise induce a strong risk of creating defects inside the particleboards. In order to study the influence of the cake moisture content, part of the cake was conditioned in a climatic chamber (25 °C, 60% RH) until the desired moisture content was attained. Moisture contents of intermediate and high moisture cake samples were  $6.2 \pm 0.1\%$  and  $8.3 \pm 0.1\%$ , respectively. A dry cake quantity of 194 g was consistently applied and when the cake moisture content was varied, the wet cake quantity was adjusted accordingly. The applied pressure, molding temperature, and molding time were varied between 19.6 and 39.2 MPa (i.e., 200–400 kgf/cm<sup>2</sup>), 155 and 205 °C, and 60 and 300 s, respectively. The resulting particleboards were conditioned in a climatic chamber (25 °C, 60% RH) for 4 weeks prior to determinations of their mechanical properties and water sensitivity.

### Post-Treatments

Coatings applied to the boards after thermopressing as a post-treatment include a coating of polyurethane varnish, product "Vernis Bateau" (Groupe V33, Domblans, France), and a linseed oil-based coating consisting of a mixture of 75% linseed oil (Onyx, Ardéa Groupe, Saint-Denis, France) and 25% turpentine (Onyx, Ardéa Groupe, Saint-Denis, France) with an added hardener (Onyx, Ardéa Groupe, Saint-Denis, France) in an amount of 30 mL/L. A heat treatment applied to the boards as an alternative post-treatment was conducted in a ventilated oven and consisted of a temperature gradient of 25–200 °C at 7.5 °C/min and 10 min at 200 °C.

### Flexural Properties

Flexural properties of the particleboards were determined according to ISO 16978:2003 with test samples of 30 mm width.<sup>28</sup> Three point flexural tests were conducted with an Instron 33R 4204 (Norwood, MA, USA) universal testing system

fitted with a 500 N load cell. A grip separation of 80 mm and a test speed of 2 mm/min were applied. Calculated flexural properties include flexural strength ( $\sigma_f$ , MPa), modulus of elasticity ( $E_f$ , GPa), breaking load ( $F_{max}$ , N), and energy-to-break ( $U$ , mJ). The latter was calculated through the area under the load deformation curve from zero to fracture. All determinations were carried out through four repetitions.

### Internal Bond Strength

The tensile strength perpendicular to the plane of the panel, or internal bond strength, was determined according to ISO 16984:2003.<sup>29</sup> Test samples were square with a side length of 50 mm. Tests were conducted by the use of an Instron 33R 4204 (Norwood, MA, USA) universal testing system, to which a 5000 N load cell and a test speed of 5 mm/min were applied. Determinations were carried out in quadruplicate.

### Charpy Impact Properties

Charpy impact properties of the unnotched test samples (60 mm  $\times$  15 mm) were assessed according to ISO 179-1:2010 by the use of a Testwell Wolpert (Gennevilliers, France) 0–40 daN cm Charpy testing apparatus.<sup>30</sup> Analyses were carried out at 23 °C and the distance between the anvils was 30 mm. This rendered the absorbed energy ( $W$ , mJ) and impact resilience ( $K$ , kJ/m<sup>2</sup>). All determinations were made through eight repetitions.

### Shore D Surface Hardness

Determination of the Shore D surface hardness of the particleboards was carried out according to ISO 868:2003 and by the use of a Bareiss (Oberdischingen, Germany) durometer.<sup>31</sup> All measurements were conducted through 32 repetitions.

### Dynamic Mechanical Thermal Analysis

Dynamic mechanical thermal analysis (DMTA) was conducted by the use of a Triton Technology Tritec 2000 (Grantham, UK) analyzer. Samples of 10 mm width and 30 mm length were applied. Measurements were made using the two point bending technique: 1 Hz frequency, 50  $\mu$ m displacement, and a 3 °C/min heating rate over a range of –50 to 165 °C. Distance between the two points was 10 mm. The analysis was carried out through four repetitions.

### Water Sensitivity

Water sensitivity of the particleboards was assessed through the determination of their thickness swelling (TS, %) and water absorption (WA, %). For this, 50 mm  $\times$  50 mm test specimens were immersed in distilled water at 20 °C for 24 h. Thickness swelling was determined according to ISO 16983:2003,<sup>32</sup> while water absorption was determined gravimetrically with an accuracy of 1 mg. All determinations were carried out through four repetitions.

### Color Characteristics

Color determinations of the particleboards were carried out with a Konica Minolta CR-410 (Tokyo, Japan) colorimeter, equipped with a pulsed xenon lamp and six silicon photocells. Results are expressed in the CIE  $L^*a^*b^*$  color space, with  $L^*$  representing lightness and varying from 0 (black) to 100 (white),  $a^*$  representing hue on the green (–) to red (+) axis and  $b^*$  representing hue on the blue (–) to yellow (+) axis. In addition, the color difference ( $\Delta E$ ) was calculated according to

**Table II.** Optimization Parameters for the Multi-objective Genetic Algorithm

Algorithm	Controlled elitist genetic algorithm
Crossover fraction	0.8
Mutation rate	Adaptive feasible
Selection	Tournament ( $k = 2$ )
Population	50
Generations	300
Pareto fraction	0.35

CIE76, where  $\Delta E = [(L_0^* - L^*)^2 + (a_0^* - a^*)^2 + (b_0^* - b^*)^2]^{1/2}$ , and where  $L_0^*$ ,  $a_0^*$ , and  $b_0^*$  are the color parameters of the particleboard obtained with thermopressing conditions from the center of the plane of experiments. All analyses were carried out through 12 repetitions.

### Experimental Design and Data Analysis

The design of experiments was carried out through a Doehlert design matrix comprising three variables: applied pressure ( $X_1$ ; 5 levels), molding time ( $X_2$ ; 7 levels), and molding temperature ( $X_3$ ; 3 levels). The center of the experimental matrix was repeated four times, leading to a total set of 16 trials. Experimental data for each response (density, mechanical properties, water sensitivity, and color characteristics) were modeled through a quadratic polynomial model by the use of the MATLAB 8.4 software package (The Mathworks Inc., Natick, MA, USA). Responses ( $y_k$ ) are expressed as follows:

$$y_k = a_0 + \sum_{i=1}^3 a_i x_i + \sum_{i=1}^3 a_{ii} x_i^2 + \sum_{\substack{i=1 \\ i \neq j}}^3 \sum_{j=2}^3 a_{ij} x_i x_j$$

where  $x_i$  and  $x_j$  represent the coded values for the independent variables, ranging from  $-1.0$  to  $1.0$ , and  $a_0$ ,  $a_i$ ,  $a_{ii}$ , and  $a_{ij}$  represent the regression coefficients obtained through regression analysis. Multi-objective optimization was carried out using a genetic algorithm, in particular a controlled elitist non-dominated sorting genetic algorithm (Table II), and taking into account the modulus of elasticity, flexural strength, and thickness swelling. The selection of these response variables was based on their use in official standards for performance requirements for the

classification of particleboards.<sup>33,34</sup> The optimal solution was next selected from a generated set of Pareto solutions.

All data obtained from experimental determinations are expressed as the mean  $\pm$  the standard deviation. Means of board characteristics for varying cake moisture content were compared by the use of a one-way analysis of variance (ANOVA) using the GLM procedure of the SAS data analysis software (Cary, NC, USA). The comparison between different individual means was performed by the use of Duncan's multiple range test at a 5% probability level.

## RESULTS AND DISCUSSION

### Physico-Chemical Characterization of the Press Cake

The press cake used as a raw material for the production of particleboards was deoiled prior to thermopressing and its composition is presented in Table I. It consisted of a fine powder composed of almost spherical particles. Through optical granulometry, the particle size distribution of the deoiled press cake was set up and is presented in Figure 1. The mean particle diameter was determined as  $54.6 \mu\text{m}$ . The deoiled cake is rich in proteins (27%) and contains only 1% of lignins. Therefore, the self-bonding character of the cake may be mainly attributed to the protein fraction. Furthermore, it has been shown that during twin-screw extrusion, proteins are almost completely denatured.<sup>35</sup> This results from the severe process conditions of twin-screw extrusion, including the intense shearing/mixing action of the extruder, particularly at the level of the reverse screw elements. This converts polymeric raw materials from their native bodies into a continuous melt and leads to structural modifications, in particular denaturation, of the protein fraction.<sup>36</sup> The resulting unordered structure facilitates protein mobilization during thermopressing and thus leads to an improved fiber wetting.

The press cake was subjected to a thermogravimetric analysis (TGA) and the degradation curve is shown in Figure 2. There is an initial mass loss at about  $100^\circ\text{C}$  which corresponds to water evaporation. The moisture content of the press cake after conditioning at 60% RH and  $25^\circ\text{C}$  was about 7% and this corresponds to the observed initial mass loss. A first thermal degradation stage is situated between  $205$  and  $375^\circ\text{C}$  and represents a 57% weight loss of the sample. It consists of the

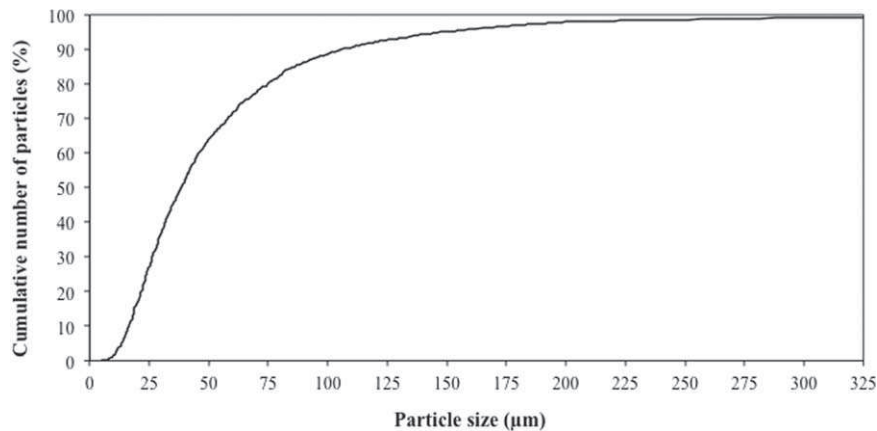


**Figure 1.** Cumulative particle size distribution for the deoiled coriander press cake.



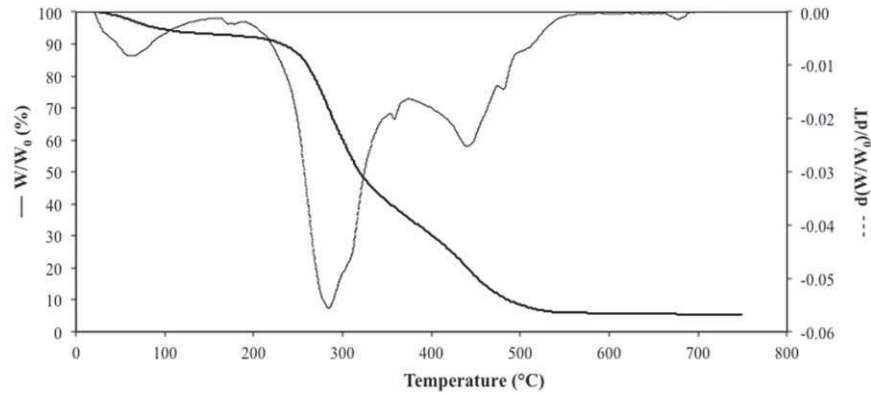


Figure 2. Thermogravimetric analysis of the deoiled coriander press cake.

simultaneous degradation of different classes of compounds, typically including cellulose, hemicelluloses and proteins.<sup>9,10,37</sup> A second degradation stage is found between 380 and 540 °C (28% of the sample weight) and is often attributed to the degradation of lignins.<sup>10,20</sup> However, the press cake composition (Table I) shows that the amount of lignins represents less than 1% of the cake on a wet weight basis. Furthermore, the 57% weight loss from the first degradation stage is significantly lower than the sum of the mass fractions of cellulose, hemicelluloses, and proteins in the cake (92%). Therefore, as thermogravimetric analyses were carried out under air atmosphere, the second degradation stage may also involve the oxidation of primary degradation products, which resulted from the degradation of the cellulose, hemicellulose, and protein fraction.<sup>11</sup> At the end of the analysis, a residual weight of about 5.5% was found, which corresponds to the mineral matter of the sample.

In this study, the mold temperature during thermopressing was varied between 155 and 205 °C. The upper limit of the temperature range was chosen based on TGA data, as degradation

would occur above 205 °C. The lower limit was set to 155 °C in order to allow the proteins to reach a rubbery state and allow effective fiber wetting. Temperatures below the glass transition temperature ( $T_g$ ) would not allow effective protein mobilization and thermopressing under such conditions would only lead to material densification. DSC analysis of the press cake revealed a glass transition temperature of 162 °C under atmospheric pressure. As thermopressing is carried out under high pressure, the proteins were estimated to reach a rubbery state at about 155 °C.

#### Influence of Thermopressing Conditions on Binderless Board Characteristics

An experimental matrix with a total of 16 trials (Table III) was set up and varies the applied pressure (19.6–39.2 MPa, corresponding to 200–400 kgf/cm<sup>2</sup>), the molding time (60–300 s), and the molding temperature (155–205 °C). The same batch of press cake was used for all trials and it was dried for 12 h at 50 °C before thermopressing, leading to a moisture content of  $3.1 \pm 0.1\%$ . The amount of cake used for thermopressing was

Table III. Experimental Matrix of Thermopressing Conditions for the Production of Binderless Boards from a Deoiled Coriander Press Cake

Board number	$X_1$	Applied pressure (MPa)	$X_2$	Molding time (s)	$X_3$	Mold temperature (°C)
1	1.000	39.2	0.000	180	0.000	180
2	-1.000	19.6	0.000	180	0.000	180
3	0.500	34.3	0.866	284	0.000	180
4	-0.500	24.5	-0.866	76	0.000	180
5	0.500	34.3	-0.866	76	0.000	180
6	-0.500	24.5	0.866	284	0.000	180
7	0.500	34.3	0.289	215	0.816	200
8	-0.500	24.5	-0.289	145	-0.816	160
9	0.500	34.3	-0.289	145	-0.816	160
10	0.000	29.4	0.577	249	-0.816	160
11	-0.500	24.5	0.289	215	0.816	200
12	0.000	29.4	-0.577	111	0.816	200
13	0.000	29.4	0.000	180	0.000	180
14	0.000	29.4	0.000	180	0.000	180
15	0.000	29.4	0.000	180	0.000	180
16	0.000	29.4	0.000	180	0.000	180

200 g or 889 mg/cm<sup>2</sup>, resulting in boards with a thickness ranging from 6.4 to 7.2 mm. All produced binderless boards were cohesive, owing to the presence of proteins as an internal binder, while the entanglement of lignocellulosic fibers provided reinforcement.<sup>20</sup>

The density, mechanical properties, which include bending properties, impact strength and surface hardness, water sensitivity, and color characteristics of the resulting binderless board materials were evaluated and are presented in Table IV. Quadratic polynomial models were fitted to the obtained data for each response and the resulting coefficients, as well as the *R*-squared values, are shown in Table V. All response models show an *R*-squared value of more than 0.85, which means that the models show satisfactory agreement with the experimental data points. Surface plots for board density, bending strength, elastic modulus, and thickness swelling are presented in Figures 3–6, respectively.

The density of the manufactured binderless boards was always high and ranged from 1230 to 1324 kg/m<sup>3</sup>. From the surface plots for board density (Figure 3), it is clear that higher densities are obtained with an increased mold temperature and molding time. This is confirmed by the model coefficients, where the mold temperature exerts the highest impact and the pressure shows a relatively low value. An increase in temperature leads to a decrease in the viscosity of the protein melt during molding, which in turn results in an improved fiber wetting and a reduced board porosity. Furthermore, the board density directly influences its mechanical properties and better mechanical resistance is obtained with boards of a higher density. The binderless board showing the highest density (Board 11) therefore also exhibits the best mechanical properties (Table IV). Further, a strong negative influence is found when both the mold temperature and pressure are high, which can also be observed in the surface plot. With such intensive molding conditions, it is not excluded that degradation, even partial, of some organic compounds, in particular proteins, has occurred within the particleboard, thus leading to a reduction in its mechanical performance.

The flexural properties of the binderless boards are represented by the flexural strength ( $\sigma_f$ , Figure 4) and the modulus of elasticity ( $E_f$ , Figure 5). They are influenced to a high degree by the thermopressing conditions and range from 4.5 to 17.9 MPa and from 1.2 to 3.7 GPa, respectively. As for the board density, the mold temperature is the most important parameter, while the molding time also exerts a great influence and the pressure shows very little influence. The same tendencies were found for the Shore D surface hardness, ranging from 68 to 79 and the Charpy impact resistance, ranging from 0.7 to 1.5 kJ/m<sup>2</sup>. The impact resistance of the manufactured binderless boards is always relatively low and shows little variation with the thermopressing conditions. This was also observed for boards produced from a sunflower cake and may be explained by the high rigidity of the boards, further shown by the obtained high elastic moduli.<sup>20</sup>

The water sensitivity of the manufactured boards is directly dependent on their porosity, which in turn is dependent on

their density. A higher density implicates a decreased porosity and this can also be seen from the moisture content of the boards (Table IV). Lower board densities, which are the case for e.g. Boards 9 and 10, are accompanied by slightly increased moisture contents. This results from their increased porosity, allowing a higher water uptake during conditioning at 25 °C and 60% RH. This elevated porosity further leads to a more important water sensitivity of the boards. The thickness swelling of the boards varies widely from 47 to 248% and the surface plots are presented in Figure 6. The mold temperature is shown to be the most influential parameter and this is related to the enhanced protein adhesivity, compatibility, and distribution among the surface of the lignocellulosic fibers with an increased temperature.<sup>12</sup> It is further shown that a longer molding time reduced the water sensitivity, which may be explained by the time necessary for the proteins to reach a complete rubbery state and to ensure proper fiber wetting.

In order to identify the optimal thermopressing conditions, a multiobjective optimization was carried out taking into account the flexural strength ( $\sigma_f$ ), the modulus of elasticity ( $E_f$ ), and the thickness swelling (TS). The choice of these three parameters was based on the ISO norm for particleboard classification, where they are used as requirements for the board properties.<sup>33</sup> The optimal conditions were further selected from a set of Pareto optimal solutions and consist of an applied pressure of 21.6 MPa ( $X_1$ : -0.81), a molding time of 300 s ( $X_2$ : 1.00), and a molding temperature of 205 °C ( $X_3$ : 1.00). With a temperature and molding time that are at the upper limit of the design matrix, the mechanical properties and water resistance of the binderless boards are maximized. Furthermore, the applied pressure is kept relatively low, which facilitates the transfer to a large-scale industrial process.

A binderless board was manufactured using these optimal conditions in order to evaluate its properties and validate the predictive power of the model. The predicted values for the board characteristics and their experimental counterparts are presented in Table VI. Next to this, the internal bond strength of the optimal board was analyzed and reached a value of  $0.68 \pm 0.03$  MPa, indicating good internal cohesion of the binderless board. A good agreement is found between the predicted and experimental values for the board density, flexural properties, and surface hardness, with the experimental values always representing more than 90% of the predicted properties. The impact properties were underestimated by about 20%, which resulted from their relatively low values throughout the model and little influence from thermopressing parameters. Next to this, the water sensitivity of the boards was strongly underestimated. This resulted from an exaggeration of the response curve, which was due to an overestimation of the water sensitivity properties of the boards produced at only 160 °C. As these boards showed almost no water resistance, issues were encountered during the determination of water absorption and thickness swelling and these values were probably overestimated. In conclusion, the model shows good predictive power for the mechanical properties of the boards, rendering it industrially valuable. However, it was shown less suitable as a predictor for water sensitivity.



**Table IV.** Characteristics of Binderless Boards Produced from a Deoiled Coriander Press Cake with Varying Thermopressing Conditions

	Board 1	Board 2	Board 3	Board 4	Board 5	Board 6	Board 7	Board 8	Board 9	Board 10	Board 11	Board 12	Board 13	Board 14	Board 15	Board 16
MC (%)	5.47 ± 0.01	5.42 ± 0.14	5.54 ± 0.05	5.97 ± 0.15	5.58 ± 0.03	5.63 ± 0.11	5.57 ± 0.12	5.84 ± 0.05	6.46 ± 0.06	6.14 ± 0.04	5.63 ± 0.31	5.81 ± 0.24	5.88 ± 0.14	5.76 ± 0.01	5.71 ± 0.12	6.07 ± 0.12
Density (kg/m <sup>3</sup> )	1295 ± 32	1285 ± 30	1320 ± 10	1258 ± 10	1279 ± 8	1309 ± 27	1293 ± 25	1230 ± 10	1252 ± 28	1270 ± 13	1324 ± 24	1305 ± 22	1286 ± 15	1280 ± 28	1295 ± 18	1288 ± 12
Flexural properties																
σ <sub>f</sub> (MPa)	9.9 ± 1.1	9.5 ± 0.8	17.4 ± 1.1	6.8 ± 0.1	7.2 ± 0.7	15.6 ± 2.5	15.9 ± 0.8	5.4 ± 0.5	4.5 ± 0.1	6.5 ± 0.9	17.9 ± 1.4	14.8 ± 1.1	12.0 ± 1.2	10.5 ± 0.3	9.9 ± 1.4	10.0 ± 1.0
E <sub>f</sub> (GPa)	2.3 ± 0.2	2.2 ± 0.1	3.3 ± 0.2	1.6 ± 0.1	1.8 ± 0.2	3.0 ± 0.5	2.9 ± 0.3	1.3 ± 0.1	1.2 ± 0.1	1.6 ± 0.2	3.7 ± 0.3	3.1 ± 0.1	2.3 ± 0.2	2.4 ± 0.3	2.3 ± 0.3	2.1 ± 0.1
F <sub>max</sub> (N)	121 ± 17	115 ± 13	195 ± 6	86 ± 4	90 ± 7	183 ± 22	183 ± 17	68 ± 5	58 ± 3	82 ± 15	204 ± 20	171 ± 13	140 ± 17	131 ± 14	119 ± 17	120 ± 11
U (mJ)	50.8 ± 9.5	50.3 ± 6.7	95.3 ± 3.8	39.4 ± 3.2	38.4 ± 4.4	86.5 ± 12.5	89.1 ± 3.4	34.5 ± 4.0	25.7 ± 1.2	35.9 ± 5.1	89.2 ± 14.3	75.3 ± 9.4	71.3 ± 18.5	54.9 ± 2.4	50.3 ± 8.4	56.8 ± 16.5
Surface hardness																
Shore D (-)	74.7 ± 2.7	74.6 ± 3.0	79.2 ± 1.6	71.5 ± 4.6	74.4 ± 3.8	78.2 ± 1.6	79.5 ± 1.5	68.1 ± 3.6	69.1 ± 4.5	72.1 ± 3.2	79.0 ± 2.0	78.9 ± 1.8	77.7 ± 2.0	75.7 ± 2.6	73.5 ± 3.8	75.9 ± 2.3
Charpy impact properties																
W (mJ)	121 ± 14	106 ± 13	133 ± 14	79 ± 7	100 ± 15	131 ± 21	143 ± 16	69 ± 10	90 ± 20	83 ± 8	145 ± 10	137 ± 11	109 ± 19	120 ± 37	134 ± 27	148 ± 18
K (kJ/m <sup>2</sup> )	1.2 ± 0.1	1.1 ± 0.1	1.4 ± 0.1	0.8 ± 0.1	1.0 ± 0.2	1.4 ± 0.2	1.5 ± 0.2	0.7 ± 0.1	0.9 ± 0.2	0.9 ± 0.1	1.5 ± 0.1	1.4 ± 0.1	1.1 ± 0.2	1.2 ± 0.3	1.4 ± 0.3	1.5 ± 0.2
Water sensibility																
WA (%)	192 ± 12	177 ± 11	99 ± 6	244 ± 3	201 ± 17	107 ± 5	71 ± 5	233 ± 8	264 ± 2	201 ± 12	55 ± 4	98 ± 9	145 ± 3	146 ± 4	189 ± 8	155 ± 5
TS (%)	187 ± 11	157 ± 11	87 ± 8	199 ± 1	170 ± 11	89 ± 2	64 ± 5	204 ± 4	248 ± 2	198 ± 9	47 ± 2	68 ± 4	106 ± 2	102 ± 7	149 ± 12	131 ± 8
Color characteristics																
L*	75.0 ± 1.0	75.3 ± 0.4	73.5 ± 0.2	76.6 ± 0.5	75.8 ± 0.6	73.7 ± 0.5	71.7 ± 0.5	76.5 ± 0.4	76.6 ± 0.5	75.8 ± 0.5	71.8 ± 0.3	73.5 ± 0.4	75.0 ± 0.5	75.0 ± 0.8	75.5 ± 0.6	74.9 ± 0.4
a*	2.4 ± 0.1	2.5 ± 0.1	2.5 ± 0.1	2.6 ± 0.1	2.6 ± 0.1	2.4 ± 0.1	2.2 ± 0.1	2.4 ± 0.1	2.4 ± 0.1	2.4 ± 0.1	2.2 ± 0.1	2.5 ± 0.1	2.5 ± 0.1	2.5 ± 0.1	2.5 ± 0.1	2.5 ± 0.1
b*	6.8 ± 0.7	7.1 ± 0.3	5.7 ± 0.2	7.9 ± 0.3	7.4 ± 0.3	5.8 ± 0.4	4.2 ± 0.4	7.7 ± 0.3	7.7 ± 0.3	7.2 ± 0.4	4.3 ± 0.3	5.8 ± 0.3	6.8 ± 0.3	6.8 ± 0.5	7.1 ± 0.4	6.7 ± 0.3
ΔE	1.0 ± 0.6	0.6 ± 0.2	2.0 ± 0.3	1.9 ± 0.6	0.9 ± 0.6	1.7 ± 0.7	4.3 ± 0.6	1.7 ± 0.5	1.8 ± 0.6	0.9 ± 0.6	4.2 ± 0.4	1.9 ± 0.6	0.5 ± 0.3	0.7 ± 0.6	0.7 ± 0.4	0.5 ± 0.3

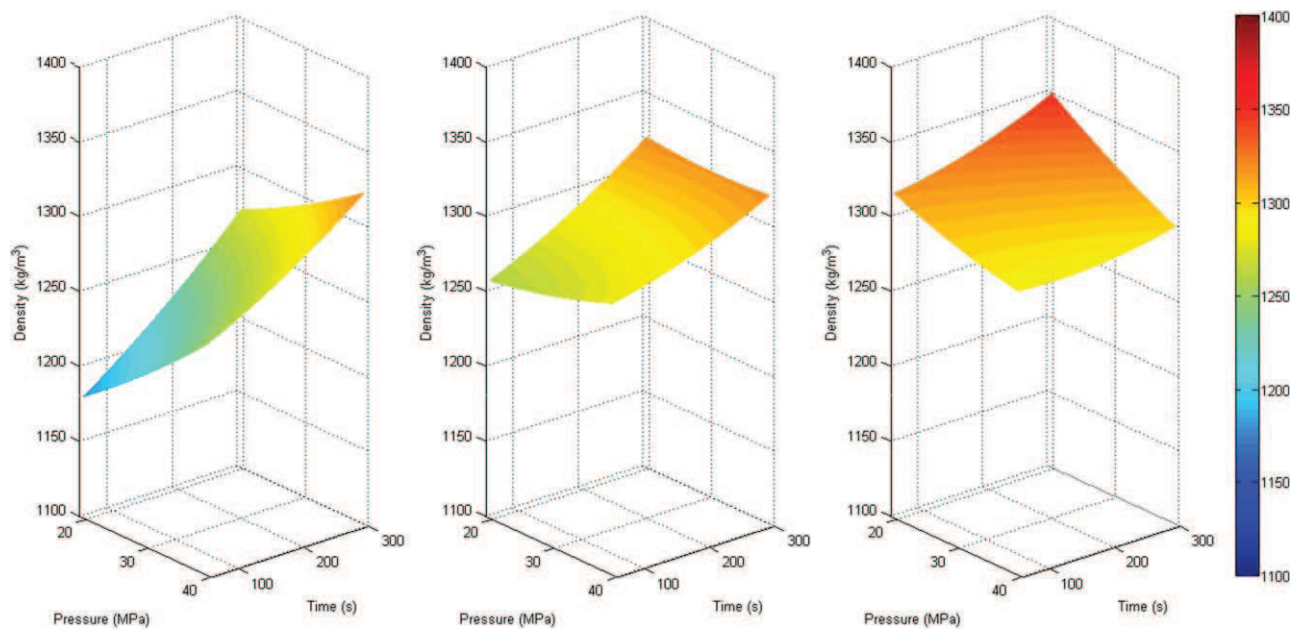


Figure 3. Surface plots for density for a mold temperature of 160, 180, and 200 °C, respectively. [Color figure can be viewed at [wileyonlinelibrary.com](http://wileyonlinelibrary.com)]

When comparing the mechanical properties of the optimal board to those resulting from the only previous study of coriander boards, using a single-screw extrusion cake,<sup>11</sup> the flexural strength and modulus of elasticity increased from 11 to 23 MPa and from 2.6 to 4.4 GPa, respectively. This represents a substantial improvement by 204 and 166%, respectively. Furthermore, the thickness swelling was reduced by 39%, decreasing from 51 to 31%. Finally, it is interesting to note that the density of the boards produced in this study was not further increased

compared to the density of the boards produced from a coriander single-screw extrusion cake (1300 kg/m<sup>3</sup>).<sup>11</sup> The improvements in mechanical properties may partly be explained by the fact that in the previous study, the press cake was not deoiled prior to thermopressing and still contained about 17% of vegetable oil. The residual oil probably led to the creation of defects inside the boards during thermopressing, as oil was expressed under high pressure. Next to this, the use of a twin-screw extrusion cake, rather a single-screw extrusion one, may result in

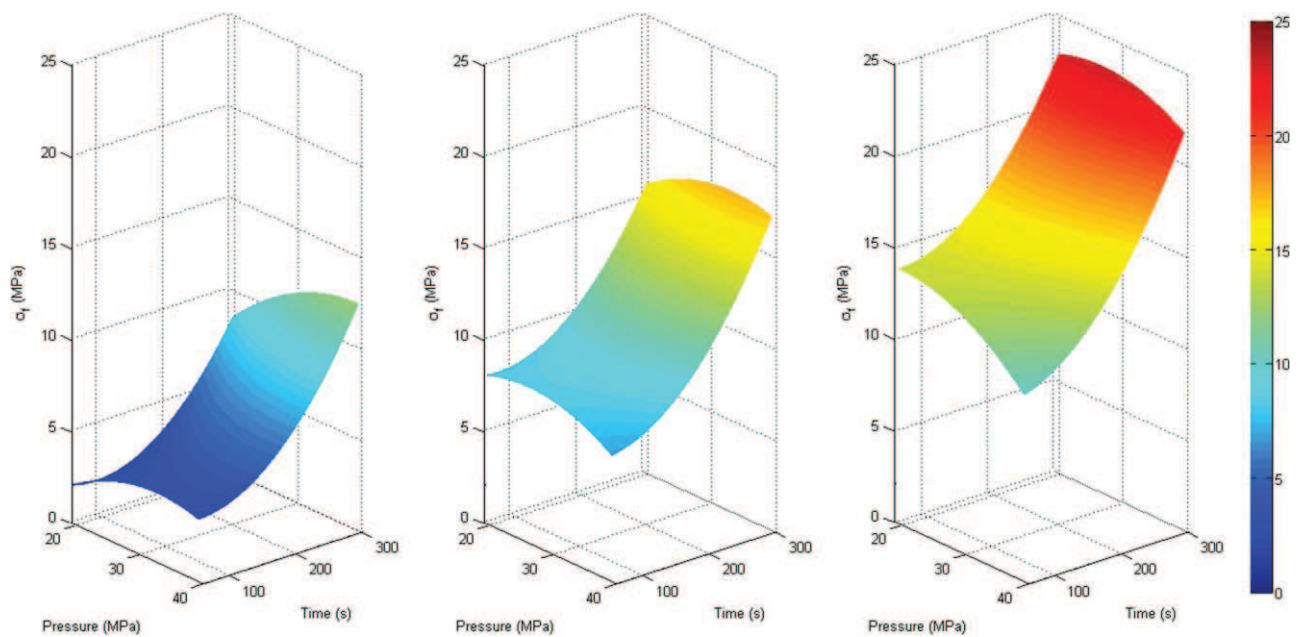
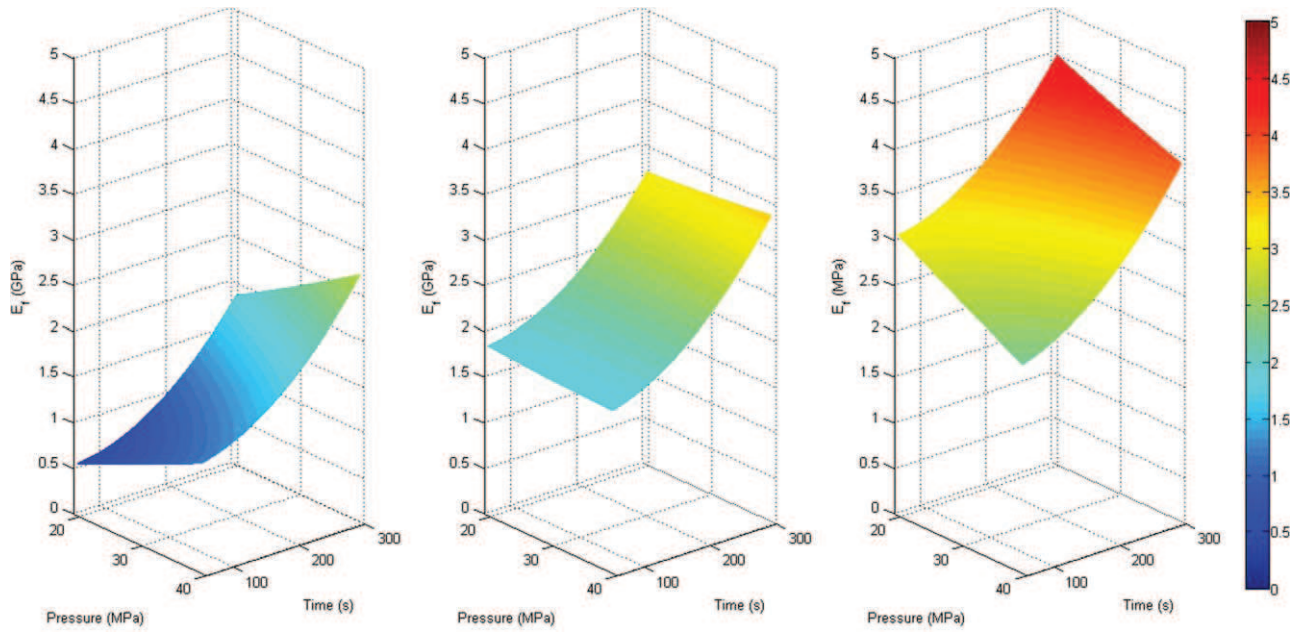


Figure 4. Surface plots for flexural strength ( $\sigma_f$ ) for a mold temperature of 160, 180, and 200 °C, respectively. [Color figure can be viewed at [wileyonlinelibrary.com](http://wileyonlinelibrary.com)]



**Figure 5.** Surface plots for modulus of elasticity ( $E_f$ ) for a mold temperature of 160, 180, and 200 °C, respectively. [Color figure can be viewed at [wileyonlinelibrary.com](http://wileyonlinelibrary.com)]

improved mechanical properties of self-bonded boards as twin-screw extrusion leads to better protein denaturation, facilitating their mobilization and fiber wetting during thermopressing.

DMTA analysis was conducted for the optimal binderless board in order to characterize its thermomechanical behavior. For comparison purposes, DMTA analysis was also performed for Board 13 and Board 10, which were thermopressed at a temperature of 180 and 160 °C, respectively (Table III), whereas the mold temperature for the optimal board was 205 °C. The

storage modulus ( $E'$ ) and the loss factor ( $\tan \delta$ ) for the different boards are presented in Figure 7 as a function of temperature. From this, it is clear that a higher mold temperature during thermopressing leads to a higher storage modulus, which confirms the presence of a stronger internal cohesion inside the binderless board when higher temperatures are applied. A first transition peak can be observed for the optimal board at a low temperature between  $-39$  and  $-36$  °C. This phenomenon may be attributed to  $\beta$ -transitions of proteins inside the board, i.e.

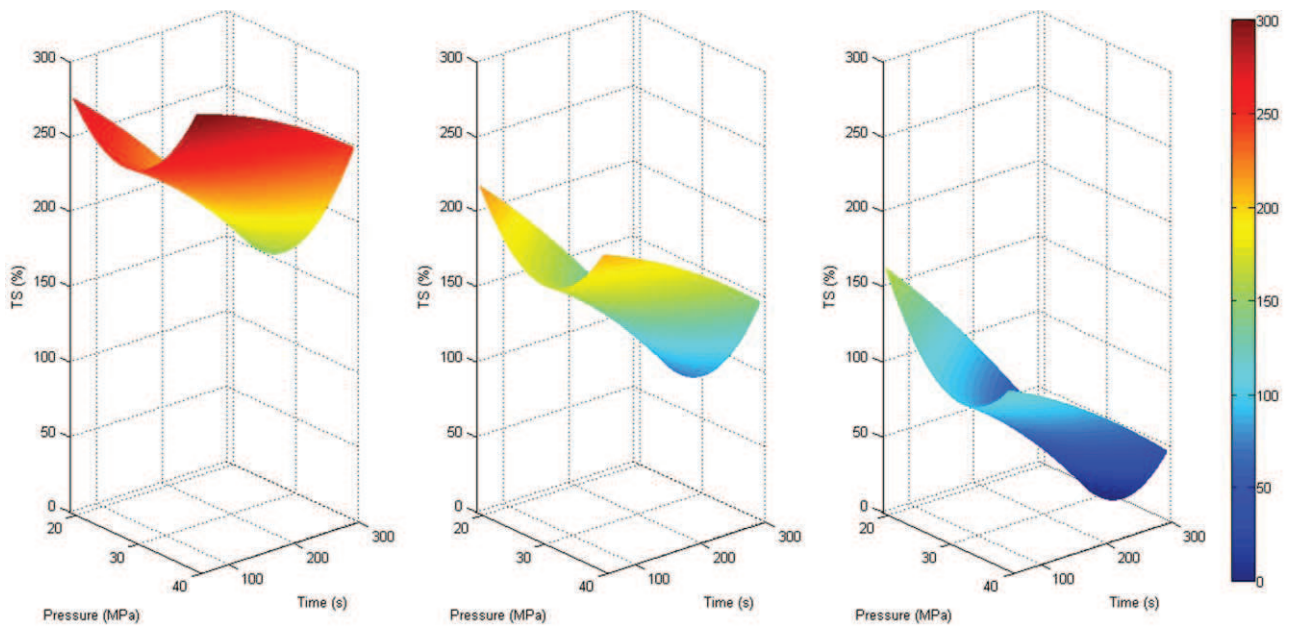


**Figure 6.** Surface plots for thickness swelling (TS) for a mold temperature of 160, 180, and 200 °C, respectively. [Color figure can be viewed at [wileyonlinelibrary.com](http://wileyonlinelibrary.com)]

**Table V.** Coefficients and R-Squared Values for the Quadratic Polynomial Models for the Characteristics of Binderless Boards Produced from a Deoiled Coriander Press Cake in Terms of the Thermopressing Conditions ( $X_1$ : applied pressure,  $X_2$ : molding time,  $X_3$ : mold temperature)

Coefficient	$a_0$	$a_1$	$a_2$	$a_3$	$a_{11}$	$a_{22}$	$a_{33}$	$a_{12}$	$a_{13}$	$a_{23}$	$R^2$
Density (kg/m <sup>3</sup> )	1287	6	25	35	3	4	-15	-6	-31	-18	0.959
Flexural properties											
$\sigma_f$ (MPa)	10.7	0.04	4.4	6.5	-0.9	2.2	-0.1	0.7	-1.5	0.8	0.926
$E_f$ (GPa)	2.3	0.02	0.7	1.1	0.01	0.3	-0.06	0.06	-0.4	0.04	0.939
$F_{max}$ (N)	127.5	0.9	48.7	72.0	-9.4	22.4	-2.7	5.4	-12.5	6.6	0.936
$U$ (mJ)	58.3	0.3	25.8	32.2	-7.8	10.7	-0.8	4.5	3.8	12.2	0.926
Shore D surface hardness											
Shore D (-)	75.7	0.7	3.0	5.8	-1.1	0.5	-1.7	-1.1	0.1	-1.7	0.938
Charpy impact properties											
$W$ (mJ)	127.5	9.2	20.1	37.6	-14.0	-17.7	-16.5	-11.6	-10.0	1.2	0.884
$K$ (kJ/m <sup>2</sup> )	1.3	0.1	0.2	0.4	-0.2	-0.2	-0.2	-0.1	-0.1	-0.01	0.896
Water sensibility											
WA (%)	159.8	3.3	-63.7	-96.9	24.6	-4.4	-14.5	19.6	-16.7	-1.5	0.946
TS (%)	130.1	11.2	-47.5	-96.2	42.1	-6.1	2.7	15.1	-21.7	-5.7	0.894
Color characteristics											
$L^*$	75.1	-0.2	-1.5	-2.4	0.07	-0.3	-1.1	0.3	-0.2	-0.8	0.990
$a^*$	2.5	-0.03	-0.1	-0.1	-0.01	0.03	-0.2	0.05	-0.05	-0.2	0.977
$b^*$	6.8	-0.2	-1.1	-1.7	0.08	-0.2	-1.0	0.2	-0.1	-0.8	0.993
$\Delta E$	0.6	0.05	0.4	1.2	0.2	1.3	2.4	0.7	-0.3	2.7	0.974

mobilization of the protein side groups.<sup>35,38</sup> No significant transition occurred between -35 and 90 °C for Board 10, up to 100 °C for Board 13, and up to 140 °C for the optimal board. Thus, no phase change took place in this temperature range, with proteins still ensuring board cohesion and the entanglement of lignocellulosic fibers serving as reinforcement. Then, a rapid decrease in the storage modulus was observed, and at the same time a peak appeared in the DMTA loss factor ( $\tan \delta$ ) curve (Figure 7). Much more significant than the first one, this second transition was associated with the  $\alpha$ -transition of the proteins, i.e. the glass transition of the protein's main chain. The corresponding temperature was around 125 °C for Board 10, around 135 °C for Board 13, and about 147 °C for the optimal board. The difference between these temperatures may be explained through the difference in moisture content (6.1, 5.9, and 5.4% for Board 10, Board 13, and the optimal board, respectively) after conditioning of the binderless boards produced at different mold temperatures, further illustrating the plasticizing effect of moisture on the protein fraction. For the optimal board, this temperature correlates well to the glass transition temperature of 148 °C that was obtained through DSC for the deoiled press cake in the same moisture content range as the optimal board (6.2% for the cake instead of 5.4% for the optimal board). And logically, as board cohesion was no longer maintained by the protein-based resin beyond this protein glass transition temperature, the storage modulus became negligible at higher temperatures.

**Table VI.** Predicted and Experimental Values for the Characteristics of a Binderless Board Produced from a Deoiled Coriander Press Cake under Optimized Thermopressing Conditions (21.6 MPa Applied Pressure, 300 s Molding Time, 205 °C Mold Temperature)

	Predicted	Experimental <sup>a</sup>
Density (kg/m <sup>3</sup> )	1345	1323 (98.4%)
Flexural properties		
$\sigma_f$ (MPa)	24.4	23.1 (94.4%)
$E_f$ (GPa)	4.7	4.4 (93.1%)
$F_{max}$ (N)	273	264 (96.5%)
$U$ (mJ)	126	120 (94.8%)
Shore D surface hardness		
Shore D (-)	81.1	79.8 (98.3%)
Charpy impact properties		
$W$ (mJ)	153	181 (118.6%)
$K$ (kJ/m <sup>2</sup> )	1.6	1.9 (119.6%)
Water sensibility		
WA (%)	-10.0	28.4
TS (%)	1.3	31.4
Color characteristics		
$L^*$	69.0	68.5 (99.3%)
$a^*$	2.0	2.0 (101.7%)
$b^*$	2.1	2.4 (114.1%)
$\Delta E$	8.3	8.1 (97.2%)

<sup>a</sup> Values in parentheses present the ratio of the experimentally obtained value to the predicted value of the response parameter.



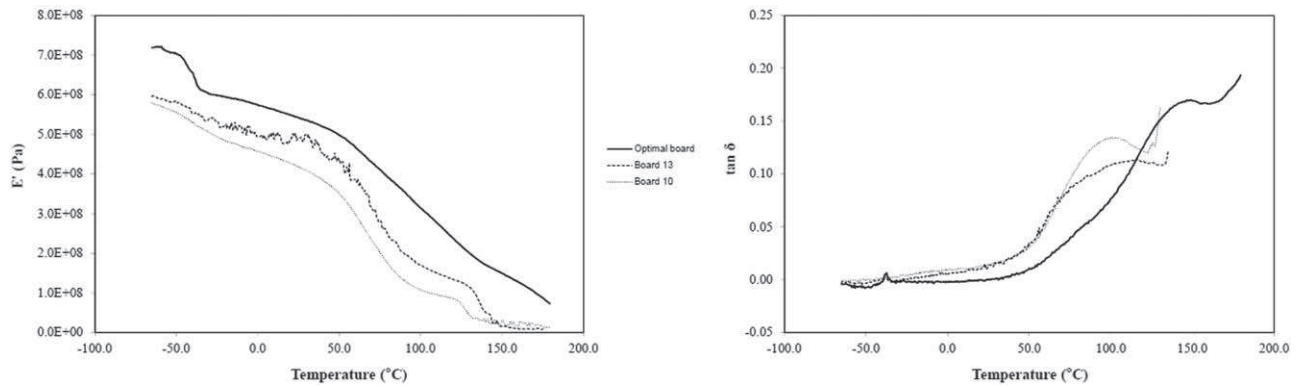


**Figure 7.** Dynamic mechanical thermal analysis of the optimal binderless board, Board 13 and Board 10: storage modulus ( $E'$ ) and loss factor ( $\tan \delta$ ) versus temperature.

High water sensitivity is a common issue for materials consisting of vegetable matter and may limit their applications in the building industry.<sup>39</sup> Even though the board produced under optimal thermopressing conditions shows relatively low water sensitivity (31% TS), different post-treatments were evaluated in order to render the binderless boards more water resistant. These include the application of a coating of linseed oil, a drying oil, or polyurethane varnish. The resulting thickness swelling of the coated boards was  $74.4 \pm 8.2\%$  and  $28.0 \pm 2.6\%$ , respectively, and did thus not undergo any significant decrease when compared to the thickness swelling of the untreated board ( $31.4 \pm 1.6\%$ ). Next to this, a heat treatment was applied at  $200^\circ\text{C}$  and was shown effective as a post-treatment to reduce water sensitivity, significantly lowering the thickness swelling to  $19.7 \pm 0.5\%$ . In order to assess the impact that such heat treatment may exert on the mechanical properties of the board, the flexural properties of the heat-treated boards were determined. The boards showed a flexural strength of  $26.7 \pm 2.3$  MPa and a modulus of elasticity of  $4.8 \pm 0.2$  GPa, leading to the conclusion that the applied heat treatment did not induce any degradation

phenomenon but further improved the boards' flexural properties. This improvement (16 and 9% for flexural strength and modulus of elasticity, respectively) may result from an improved binding effect of the protein fraction inside the board. As the heat treatment at  $200^\circ\text{C}$  probably led to the evaporation of water molecules, the establishment of hydrogen bonds between the proteins and the cellulose hydroxyl groups would be facilitated, resulting in an enhanced protein binding effect. However, it must be noted that such materials show very high rigidity, with a modulus of elasticity close to 5 GPa.

The manufactured binderless boards could find applications in the materials industry as alternatives to particleboards for use in dry conditions. According to the ISO classification, these include particleboards for general use, furniture grade, load bearing, and heavy-duty load bearing particleboards, with the latter being the most restrictive class.<sup>34</sup> The requirements for heavy-duty load bearing particleboards of 6–13 mm consist of a bending strength of 20 MPa, a modulus of elasticity of 3.1 GPa, an internal bond strength of 0.60 MPa, and a thickness swelling of 16%. In terms of mechanical properties, the optimal board

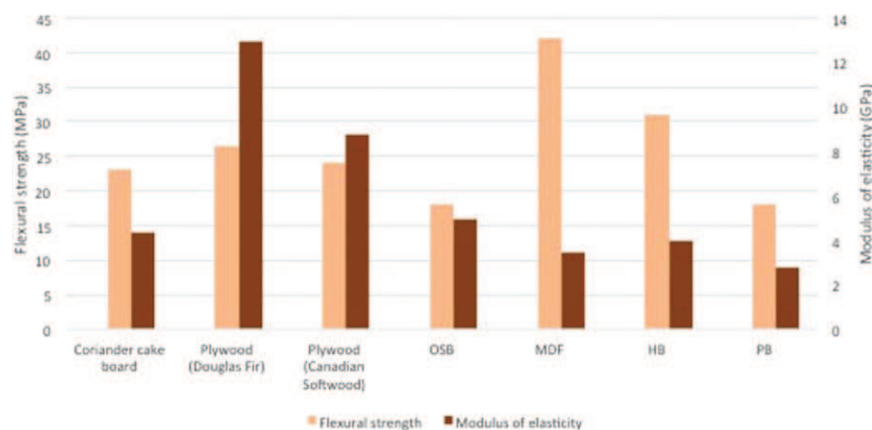


**Figure 8.** Comparison of a coriander binderless board with commercial materials. Plywood: CANPLY (Canada), unsanded Douglas Fir Plywood: 7.5 mm,  $460 \text{ kg/m}^3$ , unsanded Canadian Softwood Plywood: 7.5 mm,  $420 \text{ kg/m}^3$ . OSB (oriented strand board): EGGER (Austria), OSB 3, 6–10 mm,  $600 \text{ kg/m}^3$ . MDF (medium-density fiberboard): WoodSolutions (Australia), Standard MDF, 6–12 mm,  $775 \text{ kg/m}^3$ . HB (hardboard): Stimson Lumber Company (USA), Standard Hardboard, 6.35 mm,  $945 \text{ kg/m}^3$ . PB (particleboard): WoodSolutions (Australia), Standard Particleboard, <12 mm,  $660\text{--}700 \text{ kg/m}^3$ . [Color figure can be viewed at [wileyonlinelibrary.com](http://wileyonlinelibrary.com)]



**Table VII.** Characteristics of Binderless Boards Produced from a Deoiled Coriander Press Cake with Varying Moisture Content

Cake moisture content (%)	3.4 ± 0.1	6.2 ± 0.1	8.3 ± 0.1
Density (kg/m <sup>3</sup> )	1323 ± 1 <sup>a</sup>	1324 ± 8 <sup>a</sup>	1311 ± 8 <sup>a</sup>
Flexural properties			
σ <sub>f</sub> (MPa)	23.1 ± 0.5 <sup>a</sup>	25.8 ± 6.3 <sup>a</sup>	24.1 ± 6.9 <sup>a</sup>
E <sub>f</sub> (GPa)	4.4 ± 0.1 <sup>a</sup>	3.9 ± 0.8 <sup>a</sup>	4.0 ± 0.9 <sup>a</sup>
F <sub>max</sub> (N)	264 ± 6 <sup>a</sup>	283 ± 81 <sup>a</sup>	266 ± 84 <sup>a</sup>
U (mJ)	120 ± 2 <sup>a</sup>	170 ± 37 <sup>a</sup>	140 ± 38 <sup>a</sup>
Shore D surface hardness			
Shore D (–)	79.8 ± 1.2 <sup>a</sup>	80.2 ± 1.2 <sup>a,b</sup>	80.5 ± 0.9 <sup>b</sup>
Charpy impact properties			
W (mJ)	181 ± 13 <sup>a</sup>	196 ± 35 <sup>a</sup>	205 ± 20 <sup>a</sup>
K (kJ/m <sup>2</sup> )	1.9 ± 0.2 <sup>a</sup>	2.1 ± 0.3 <sup>a,b</sup>	2.2 ± 0.2 <sup>b</sup>
Water sensibility			
WA (%)	28.4 ± 1.8 <sup>a</sup>	24.5 ± 4.3 <sup>a</sup>	24.5 ± 2.8 <sup>a</sup>
TS (%)	31.4 ± 1.6 <sup>a</sup>	31.8 ± 6.8 <sup>a</sup>	30.1 ± 2.0 <sup>a</sup>
Color characteristics			
L*	68.5 ± 0.5 <sup>a</sup>	67.7 ± 0.5 <sup>b</sup>	67.2 ± 0.2 <sup>c</sup>
a*	2.0 ± 0.2 <sup>a</sup>	1.7 ± 0.2 <sup>b</sup>	1.5 ± 0.1 <sup>c</sup>
b*	2.4 ± 0.5 <sup>a</sup>	1.6 ± 0.5 <sup>b</sup>	1.1 ± 0.2 <sup>c</sup>
ΔE	8.1 ± 0.6 <sup>a</sup>	9.0 ± 0.6 <sup>b</sup>	9.8 ± 0.3 <sup>c</sup>

Means in the same row with the same superscript letter (a-c) are not significantly different at  $P < 0.05$ .

meets the requirements well (23.1 MPa flexural strength, 4.4 GPa modulus of elasticity, and 0.68 MPa internal bond strength). However, it shows an excessive thickness swelling of 31% and even when the board had undergone a heat treatment after thermopressing, the 16% requirement was not met (20% TS). For load-bearing particleboards, this thickness swelling requirement is fixed at 19%. Applications for this class of boards include domestic flooring, shelving, and general construction.<sup>34</sup> With the application of a post-treatment, the produced binderless boards of this study show high potential to meet these requirements and thus acts as a more sustainable alternative to conventional particleboards. However, further research is necessary to optimize the board post-treatments in order to reduce their water sensitivity.

A comparison of the flexural properties of the optimal board with several commercial boards is presented in Figure 8. From this, it is shown that the bending properties of a binderless board produced from a deoiled coriander twin-screw extrusion cake are comparable to those of a commercial wood-based material such as oriented strand board (OSB) and are superior to the bending properties of a commercial particleboard (PB). Furthermore, the manufactured binderless boards do not involve the use of any adhesives, rendering them safer in terms of harmful emissions, in particular formaldehyde, and significantly more environmentally friendly. However, it must be noted that the boards from this study show a significantly higher density (1323 kg/m<sup>3</sup>) than most commercial boards which could result in difficulties in handling and transportation. The relatively high panel density is a result of the absence of synthetic resins and similar high densities were obtained for other

binderless boards, such as panels produced from sunflower cake (1267 kg/m<sup>3</sup>) or date palm lignocellulosic by-products (around 1000 kg/m<sup>3</sup>).<sup>20,40</sup> Further, the use of thermopressing with high temperature and pressure, necessary to mobilize the natural binder (i.e., proteins), contributes to high densities in boards.<sup>5</sup>

#### Influence of Press Cake Moisture Content on Binderless Board Characteristics

In order to evaluate the effect of moisture on the thermopressing process and the resulting boards' characteristics, the press cake moisture content was varied to levels of 3.1 ± 0.1% (i.e., the moisture content used to optimize the thermopressing conditions), 6.2 ± 0.1% and 8.3 ± 0.1%. Moisture is known to act as a plasticizer in materials and can induce polymer softening, which would lead to a reduction of the glass transition temperature ( $T_g$ ) of the polymer system. In order to validate the diluent effect of moisture in the extrusion press cake, cake samples of each moisture content level were subjected to DSC analysis. The resulting  $T_g$  was 161.7, 147.8, and 141.8 °C for a moisture content of 3.1, 6.2, and 8.3%, respectively, indicating the plasticizing effect of an increased moisture content on the press cake proteins. This phenomenon was also observed for sunflower proteins and may be explained through hydrogen linking of the polar groups of the proteins with the present moisture, reducing polymer interactions, separating the proteins, and thus facilitating their movement.<sup>41</sup>

The increased protein mobilization would enhance fiber wetting during the thermopressing process, leading to improved mechanical properties of the resulting boards. However, the increased moisture content would also lead to an increased

amount of heated water vapor generated during thermopressing. This vapor is driven toward the center of the material, where it creates a high internal mat pressure which could break the developing autoadhesive bonds and result in internal fracturing of the board.<sup>20,41</sup> In order to reduce this phenomenon, a gradual decrease of the applied platen pressure was employed at the end of the thermopressing process. Despite this measure, a significantly increased “blow” of the material was observed with opening of the press when cake with increased moisture content was used. This implies high internal pressures, potentially leading to internal fracturing of the boards.

The resulting board characteristics for the three levels of moisture content of the press cake are presented in Table VII. From this, it is clear that an increased moisture content of the cake does not lead to significant improvements in the mechanical properties or water sensitivity of the resulting self-bonded boards. This may result from the opposing factors of an enhanced fiber wetting on the one hand, and internal fracturing of the board on the other hand. Further, increased cake moisture contents seem to induce high variability of the mechanical properties. For example, in terms of the flexural strength, the coefficient of variation (i.e., the ratio of the standard deviation to the mean value) increases from 2% to 29% for a cake moisture content of 3.4 and 8.3%, respectively. This increase in variability is due to inhomogeneity of the material, which in turn is caused by internal fractures that are present inside the manufactured boards. The color characteristics of the boards, however, varied significantly with varying cake moisture content. For example, the lightness of the boards ( $L^*$ ) decreased from 68.5 to 67.2 when the moisture content of the press cake increased from 3.4 to 8.3%. This may result from increased darkening of the protein fraction at higher cake moisture contents, as the latter causes a decrease in  $T_g$  and thus a larger temperature increase between the glass transition and the thermopressing temperature.

## CONCLUSIONS

During this study, cohesive self-bonded boards were produced through thermopressing of a coriander twin-screw extrusion cake that was further deoiled. During thermopressing, the cake proteins reached a rubbery state, leading to their mobilization and the capacity to act as a natural binder inside the boards, while the lignocellulosic fibers behave as reinforcing fillers. The influence of the thermopressing operating parameters was assessed and quadratic polynomial models were set up that describe the board characteristics in terms of applied pressure, molding time, and molding temperature. Such models may be valuable for the materials industry for their predictive power of the density and mechanical properties of manufactured boards. Optimized thermopressing conditions include an applied pressure of 21.6 MPa, a molding time of 300 s, and a molding temperature of 205 °C. This resulted in a binderless board with a density of 1323 kg/m<sup>3</sup>, 23.1 MPa flexural strength, 4.4 GPa modulus of elasticity, and 31% thickness swelling. Several post-treatments were implemented in order to reduce the boards' water sensitivity and a heat treatment at 200 °C during 10 min was shown to effectively reduce thickness swelling to 20%. Next

to this, an increased moisture content of the press cake did not lead to mechanically more resistant boards and induced internal fracturing during thermopressing. The obtained binderless boards were shown to be comparable in terms of mechanical properties to commercial boards such as oriented strand board and particleboard. The coriander boards could therefore present a more sustainable alternative to these wood-based boards, further avoiding the use of chemical adhesives.

## ACKNOWLEDGMENTS

The authors would like to express their sincere gratitude to Ovalie Innovation (Auch, France) for providing financial support for the project and for supplying the coriander seeds used for the purpose of this study. Next to this, the authors would also like to thank Guadalupe Vaca Medina (Laboratoire de Chimie Agro-industrielle (LCA), Institut National Polytechnique de Toulouse) for conducting the DMTA analyses.

## REFERENCES

1. Halvarsson, S.; Edlund, H.; Norgren, M. *Ind. Crops Prod.* **2009**, *29*, 437.
2. Widyorini, R.; Xu, J.; Umemura, K.; Kawai, S. *J. Wood Sci.* **2005**, *51*, 648.
3. Hashim, R.; Said, N.; Lamaming, J.; Baskaran, M.; Sulaiman, O.; Sato, M.; Hiziroglu, S.; Sugimoto, T. *Mater. Des.* **2011**, *32*, 2520.
4. Okuda, N.; Sato, M. *J. Wood Sci.* **2004**, *50*, 53.
5. Tajuddin, M.; Ahmad, Z.; Ismail, H. *BioResources* **2016**, *11*, 5600.
6. Evon, P.; Vandenbossche, V.; Rigal, L. *Polym. Degrad. Stab.* **2012**, *97*, 1940.
7. Okuda, N.; Hori, K.; Sato, M. *J. Wood Sci.* **2006**, *52*, 244.
8. Evon, P.; Vandenbossche, V.; Pontalier, P. Y.; Rigal, L. *Ind. Crops Prod.* **2014**, *52*, 354.
9. Evon, P.; Amalia Kartika, I.; Rigal, L. *J. Renew. Mater.* **2014**, *2*, 52.
10. Hidayat, H.; Keijsers, E. R. P.; Prijanto, U.; van Dam, J. E. G.; Heeres, H. *J. Ind. Crops Prod.* **2014**, *52*, 245.
11. Uitterhaegen, E.; Nguyen, Q. H.; Merah, O.; Stevens, C. V.; Talou, T.; Rigal, L.; Evon, P. *J. Renew. Mater.* **2016**, *4*, 225.
12. Kurniati, M.; Fahma, F.; Amalia Kartika, I.; Sunarti, T. C.; Syamsu, K.; Hermawan, D.; Saito, Y.; Sato, M. *Asian J. Agric. Res.* **2015**, *9*, 180.
13. Sharma, R. P.; Singh, R. S.; Verma, T. P.; Tailor, B. L.; Sharma, S. S.; Singh, S. K. *Econ. Aff.* **2014**, *59*, 345.
14. Sahib, N. G.; Anwar, F.; Gilani, A. H.; Hamid, A. A.; Saari, N.; Alkharfy, K. M. *Phytother. Res.* **2013**, *27*, 1439.
15. Alaluf, S.; Green, M. R.; Powell, J. R.; Rogers, J. S.; Watkinson, A.; Cain, F. W.; Hu, H. L.; Rawlings, A. V. (UNILEVER N.V.). U.S. Patent 6,365,175 B1, 2 April **2002**.
16. Alaluf, S.; Hu, H. L.; Green, M. R.; Powell, J. R.; Rawlings, A. V.; Rogers, J. S. (UNILEVER N.V.). Patent EP 1,013,178 B1, 28 September **2005**.

17. Uitterhaegen, E.; Sampaio, K. A.; Delbeke, E. I. P.; De Greyt, W.; Cerny, M.; Evon, P.; Merah, O.; Talou, T.; Stevens, C. V. *Molecules* **2016**, *21*, 1202.
18. European Food Safety Authority (EFSA). *EFSA J* **2013**, *11*, 3422.
19. Uitterhaegen, E.; Nguyen, Q. H.; Sampaio, K. A.; Stevens, C. V.; Merah, O.; Talou, T.; Rigal, L.; Evon, P. *J. Am. Oil Chem. Soc.* **2015**, *92*, 1219.
20. Evon, P.; Vinet, J.; Labonne, L.; Rigal, L. *Ind. Crops Prod.* **2015**, *65*, 117.
21. John, M. J.; Thomas, S. *Carbohydr. Polym.* **2008**, *71*, 343.
22. ISO. ISO 659:2009. Oilseeds - Determination of oil content; International Organization for Standardization: Switzerland, **2009**.
23. ISO. ISO 665:2000. Oilseeds - Determination of moisture and volatile matter content; International Organization for Standardization: Switzerland, **2000**.
24. ISO. ISO 749:1977. Oilseed residues - Determination of total ash; International Organization for Standardization: Switzerland, **1977**.
25. Van Soest, P. J.; Wine, R. H. *J. Assoc. Off. Agric. Chem.* **1967**, *50*, 50.
26. Van Soest, P. J.; Wine, R. H. *J. Assoc. Off. Agric. Chem.* **1968**, *51*, 780.
27. ISO. ISO 5983-1:2005. Animal feeding stuffs - Determination of nitrogen content and calculation of crude protein content - Part 1: Kjeldahl method; International Organization for Standardization: Switzerland, **2005**.
28. ISO. ISO 16978:2003. Wood-based panels - Determination of modulus of elasticity in bending and of bending strength; International Organization for Standardization: Switzerland, **2003**.
29. ISO. ISO 16984:2003. Wood-based panels - Determination of tensile strength perpendicular to the plane of the panel; International Organization for Standardization: Switzerland, **2003**.
30. ISO. ISO 179-1:2010. Plastics - Determination of Charpy impact properties, Part 1: Non-instrumented impact test; International Organization for Standardization: Switzerland, **2010**.
31. ISO. ISO 868:2003. Plastics and ebonite - Determination of indentation hardness by means of a durometer (Shore hardness); International Organization for Standardization: Switzerland, **2003**.
32. ISO. ISO 16983:2003. Wood-based panels - Determination of swelling in thickness after immersion in water; International Organization for Standardization: Switzerland, **2003**.
33. ISO. ISO 16893-2:2010. Wood-based panels - Particleboard - Part 2: Requirements; International Organization for Standardization: Switzerland, **2010**.
34. ISO. ISO 16893-1:2008. Wood-based panels - Particleboard - Part 1: Classifications; International Organization for Standardization: Switzerland, **2008**.
35. Evon, P.; Vandenbossche, V.; Pontalier, P. Y.; Rigal, L. *Adv. Mat. Res.* **2010**, *112*, 63.
36. Bouvier, J. M.; Campanella, O. H. *Extrusion Processing Technology: Food and Non-Food Biomaterials*; Wiley: Chichester, UK, **2014**.
37. Hatakeyama, T.; Hatakeyama, H. *Thermal Properties of Green Polymers and Biocomposites*; Springer: Dordrecht, the Netherlands, **2004**.
38. Zhang, J.; Mungara, P.; Jane, J. *Polymer* **2001**, *42*, 2569.
39. Stokke, D. D.; Wu, Q.; Han, G. *Introduction to Wood and Natural Fiber Composites*; Wiley: Chichester, UK, **2013**.
40. Saadaoui, N.; Rouilly, A.; Fares, K.; Rigal, L. *Mater. Des.* **2013**, *50*, 302.
41. Rouilly, A.; Orliac, O.; Silvestre, F.; Rigal, L. *Polymer* **2001**, *42*, 10111.